

# An Efficient Algorithm for Solving the Phase Field Crystal Model

Mowei Cheng\* and James A. Warren

*Metallurgy Division and Center for Theoretical and Computational Materials Science, National Institute of Standards and Technology, 100 Bureau Drive, Stop 8554, Gaithersburg, Maryland 20899, USA*

---

## Abstract

We present and discuss how to develop an unconditionally stable algorithm for solving the Phase Field Crystal (PFC) model. This algorithm allows for an arbitrarily large algorithmic time step. In order to study the accuracy of the algorithm, we determine an effective time step in Fourier space, and use this quantity as the basis of our analysis. Comparing our calculations with a set of representative numerical results, we demonstrate that this algorithm is an effective approach for the study of the PFC models. As the PFC model is just a simple example of a wide class of density function theories, we expect this method will have wide applicability to modeling systems of considerable interest to the materials modeling communities.

*Key words:* Unconditionally stable, Phase Field Crystal model

*PACS:* 05.10.-a, 02.60.Cb, 64.75.+g, 81.15.Aa

---

## 1 Introduction

The dynamics of a non-equilibrium system often results in highly complicated domain structures (microstructures). Typically, as time proceeds, the average size of these structures grows as a direct consequence of free-energy reduction: the interface is eliminated resulting in an increase in the size of homogeneous regions. Traditional non-equilibrium dynamics usually deals with the equilibrium states that are spatially uniform [1,2,3,4], i.e., the stable phases are constant phases. Classic, albeit quite simple, examples of models governing

---

\* Corresponding author. Tel: +1-301-975-5729; Fax: +1-301-975-5012.

*Email address:* mowei.cheng@nist.gov (Mowei Cheng).

the evolution of such systems are the Cahn-Hilliard (CH) Equation for conserved systems [5] and Allen-Cahn (AC) Equation for non-conserved systems [6]. Examples are found in polymer mixtures [7], alloys [8,9], liquid-crystals [10,11], and in cosmology [12].

A model that has generated considerable recent interest is Phase Field Crystal (PFC) Equation [13,14], which is a conservative form of the familiar, non-conserved, Swift-Hohenberg (SH) Equation [15]. These systems differ from the CH and AC systems in that the stable phase are periodic. In the case of PFC model, which is a simple version of more elaborate density function theories of liquid/crystal interfaces [16,17], the model therefore represents more realistic physical properties of atomic systems such as the basic properties of polycrystalline materials in non-equilibrium processing phenomena. For SH models, the order parameter is viewed as capturing the inhomogeneities in a fluid associated with Rayleigh-Bénard convection.

The equations of motion governing these non-equilibrium phenomena are non-linear partial differential equations that cannot generally be solved analytically for random initial conditions. Therefore, computer simulations play an essential role in our understanding and characterization of non-equilibrium phenomena. The standard Euler integration is known to be unstable for time step  $\Delta t$  above a threshold fixed by lattice spacing  $\Delta x$  [18]. In CH and AC systems, to maintain an interfacial profile, the lattice spacing must be smaller than the interfacial width  $\xi$ , and in PFC and SH systems,  $\Delta x$  must smaller than the periodicity selected by the system. Thus, the Euler update is inefficient, and in practice it is computationally costly to use to evolve large systems. Various computational algorithms [19,20,21] have been developed by increasing  $\Delta t$  compared to the simplest Euler discretization. However, these methods still require a fixed time step, so they eventually become inefficient. Recently, unconditionally stable algorithms [22,23,24] were developed to overcome this difficulty for CH and AC Equations. These algorithms are a class of stable algorithms free of the fixed time step constraint for equations with a mix of implicit and explicit terms. While these algorithms allow for an increasing time step in CH systems as time proceeds, only a finite effective time step is possible for AC systems. A recent study [25], based on this unconditionally stable algorithm, demonstrated analytically that one can use an accelerated algorithm  $\Delta t = At^{2/3}$  to drive the CH Equation, and the accuracy in correlation is controlled by  $\sqrt{A}$ .

In the next part of this manuscript (Section 2) we apply this unconditionally stable algorithm to the PFC and SH Equations. Section 3 examines the effectiveness of this approach through some numerical studies of the algorithm, demonstrating that the algorithm is efficient and accurate for PFC Equation. Finally, in Section 4 we provide some concluding remarks.

## 2 Unconditionally stable algorithms for PFC Equation

In this section, we apply the unconditionally stable time stepping algorithms ( $\Delta t$  taken arbitrarily large without the solution becoming unstable) to the PFC and SH Equations. Although the main purpose of this section is to study unconditionally stable algorithms on PFC Equation, we include a parallel discussion of the SH Equation, as the methodology yields unconditionally stable algorithms on these two equations has only minor differences.

### 2.1 Unconditionally Stable Finite Differences

Both the PFC and SH Equations start from a free energy functional that describes the configurational cost of periodic phases in contact with isotropic phases, and can be expressed as

$$F[\phi] = \int d\mathbf{x} \left\{ \frac{1}{2} \phi \left[ r + (1 + \nabla^2)^2 \right] \phi + \frac{\phi^4}{4} \right\}, \quad (1)$$

where the periodic order parameter  $\phi(\mathbf{x}, t)$  has the wave number  $k_0 = 1$  in equilibrium, and  $r < 0$  is a control parameter (scaled temperature difference  $T - T_M$ ) that characterizes the quench depth.

In the PFC model the order parameter is conserved, and thus the equation of motion is in the form of a continuity equation,  $\partial\phi/\partial t = -\nabla \cdot \mathbf{j}$ , with current  $\mathbf{j} = -M\nabla(\delta F/\delta\phi)$ , where  $M$  is the mobility. Absorbing  $M$  into the time scale, we obtain the dimensionless form of the PFC Equation

$$\frac{\partial\phi}{\partial t} = \nabla^2 \frac{\delta F}{\delta\phi} = \nabla^2 \left\{ \left[ r + (1 + \nabla^2)^2 \right] \phi + \phi^3 \right\}. \quad (2)$$

For the SH Equation, on the other hand, the order parameter is not conserved by the dynamics, and the evolution of the field is postulated to have the simple dissipative form:

$$\frac{\partial\phi}{\partial t} = -\frac{\delta F}{\delta\phi} = - \left[ r + (1 + \nabla^2)^2 \right] \phi - \phi^3. \quad (3)$$

Eq. (3) describes that the rate of change of  $\phi$  is proportional to the gradient (with an an  $L^2$  inner product in functional space) of the free-energy functional.

In order to obtain an unconditionally stable algorithm, we now follow methods previously developed for the CH and AC Equations [22,23,24], and work out in

some detail how to semi-implicitly parameterize the equation of motion both for Eq. (2):

$$\begin{aligned} & \phi_{t+\Delta t} + \Delta t \nabla^2 \left[ (a_1 - 1)(r + 1)\phi_{t+\Delta t} + 2(a_2 - 1)\nabla^2 \phi_{t+\Delta t} + (a_3 - 1)\nabla^4 \phi_{t+\Delta t} \right] \\ &= \phi_t + \Delta t \nabla^2 \left[ a_1(r + 1)\phi_t + 2a_2\nabla^2 \phi_t + a_3\nabla^4 \phi_t + \phi_t^3 \right], \end{aligned} \quad (4)$$

and for Eq. (3):

$$\begin{aligned} & \phi_{t+\Delta t} - \Delta t \left[ (a_1 - 1)(r + 1)\phi_{t+\Delta t} + 2(a_2 - 1)\nabla^2 \phi_{t+\Delta t} + (a_3 - 1)\nabla^4 \phi_{t+\Delta t} \right] \\ &= \phi_t - \Delta t \left[ a_1(r + 1)\phi_t + 2a_2\nabla^2 \phi_t + a_3\nabla^4 \phi_t + \phi_t^3 \right], \end{aligned} \quad (5)$$

In order to find the constraints for the parameters  $a_1$ ,  $a_2$  and  $a_3$  for unconditionally stable algorithms, we perform a standard von Neumann linear stability analysis on Eq. (4) and Eq. (5). The procedures are quite similar and the results are identical for these two equations. Here we only show the details for the PFC model.

Substituting  $\phi = \bar{\phi} + \eta$  in Eq. (4), where  $\bar{\phi}$  is the uniform solution and  $\eta$  is a small perturbation, we get

$$\begin{aligned} & \eta_{t+\Delta t} + \Delta t \nabla^2 \left[ (a_1 - 1)(r + 1)\eta_{t+\Delta t} + 2(a_2 - 1)\nabla^2 \eta_{t+\Delta t} + (a_3 - 1)\nabla^4 \eta_{t+\Delta t} \right] \\ &= \eta_t + \Delta t \nabla^2 \left[ a_1(r + 1)\eta_t + 2a_2\nabla^2 \eta_t + a_3\nabla^4 \eta_t + 3\bar{\phi}^2 \eta_t \right], \end{aligned} \quad (6)$$

The Fourier transform the above equation gives

$$\begin{aligned} & \eta_{\mathbf{k},t+\Delta t} \left[ 1 - \Delta t k^2 \{ (a_1 - 1)(r + 1) - 2(a_2 - 1)k^2 + (a_3 - 1)k^4 \} \right] \\ &= \eta_{\mathbf{k},t} \left[ 1 - \Delta t k^2 \{ a_1(r + 1) - 2a_2k^2 + a_3k^4 + 3\bar{\phi}^2 \} \right]. \end{aligned} \quad (7)$$

Writing this as

$$\eta_{\mathbf{k},t+\Delta t} [1 + \Delta t \mathcal{L}_{\mathbf{k}}] = \eta_{\mathbf{k},t} [1 + \Delta t \mathcal{R}_{\mathbf{k}}]. \quad (8)$$

The von Neumann stability criterion requires that  $|\eta_{\mathbf{k},t+\Delta t}| < |\eta_{\mathbf{k},t}|$ , which forces the deviation from the constant phase to decrease in magnitude with time in Fourier space. We obtain

$$|1 + \Delta t \mathcal{L}_{\mathbf{k}}| > |1 + \Delta t \mathcal{R}_{\mathbf{k}}|. \quad (9)$$

Therefore we have  $\mathcal{L}_{\mathbf{k}} - \mathcal{R}_{\mathbf{k}} > 0$  and  $\mathcal{L}_{\mathbf{k}} + \mathcal{R}_{\mathbf{k}} > 0$ . The first condition yields

$$0 < k^2[(r + 3\bar{\phi}^2) + (1 - k^2)^2], \quad (10)$$

and we obtain the restriction  $r + 3\bar{\phi}^2 < 0$ . This condition has physical meaning in PFC model — it ensures that the isotropic phase  $\bar{\phi}$  is metastable while the periodic (crystalline) phase [14] is stable. In other words,  $r < -3\bar{\phi}^2$  indicates an undercooled liquid. The second inequality yields

$$0 < -k^2[(r + 1)(2a_1 - 1) + 3\bar{\phi}^2 - 2(2a_2 - 1)k^2 + (2a_3 - 1)k^4], \quad (11)$$

and a sufficient condition is

$$a_1 < \frac{1}{2} - \frac{3\bar{\phi}^2}{2(r + 1)}, \quad a_2 \geq \frac{1}{2}, \quad a_3 \leq \frac{1}{2}. \quad (12)$$

These are the constraints on the parameters  $a_1$ ,  $a_2$  and  $a_3$  for unconditionally stable algorithms for all modes. With these choices there is no threshold for  $\Delta t$  in order to maintain stability. We term  $\Delta t$  as the *algorithmic time step*. Unconditional stability does not mean that the user of such algorithms may simply take as large a time step as is desired. Indeed, to obtain accurate physical results, there are additional restrictions on how large  $\Delta t$  may be.

## 2.2 Effective time step

To determine how large a time step we may take, and still maintain an accurate solution, we calculate the Fourier space “effective time step”, as will be described below. We first note that when  $a_1 = a_2 = a_3 = 1$ , Eq. (4) corresponds to the traditional Euler update

$$\frac{\phi'_{t+\Delta t} - \phi_t}{\Delta t_{Eu}} = \nabla^2 \left\{ \left[ r + (1 + \nabla^2)^2 \right] \phi_t + \phi_t^3 \right\}, \quad (13)$$

where  $\phi'_{t+\Delta t}$  denotes the field obtained after an Euler update on a previous field  $\phi_t$ , while we use the unprimed  $\phi_{t+\Delta t}$  to denote the field obtained by unconditionally stable algorithm on  $\phi_t$  throughout.

We now define the spatial Fourier transform of  $\phi_{\mathbf{k},t} = \int d\mathbf{x} e^{-i\mathbf{k}\cdot\mathbf{x}} \phi_t(\mathbf{x})$ . In Fourier space, writing  $k^2 \equiv |\mathbf{k}|^2$ , the Euler update becomes

$$\frac{\phi'_{\mathbf{k},t+\Delta t} - \phi_{\mathbf{k},t}}{\Delta t_{Eu}} = -k^2 \left\{ \left[ r + (1 - k^2)^2 \right] \phi_{\mathbf{k},t} + (\phi^3)_{\mathbf{k},t} \right\}, \quad (14)$$

where  $(\phi^3)_{\mathbf{k},t} = \int d\mathbf{x} e^{-i\mathbf{k}\cdot\mathbf{x}} \phi_t^3(\mathbf{x})$ .

In Fourier space, the unconditionally stable algorithms Eq. (4) can be written in a form that is analogous to Eq. (14):

$$\frac{\phi_{\mathbf{k},t+\Delta t} - \phi_{\mathbf{k},t}}{\Delta t_{eff}^{PFC}(k, \Delta t)} = -k^2 \left\{ \left[ r + (1 - k^2)^2 \right] \phi_{\mathbf{k},t} + (\phi^3)_{\mathbf{k},t} \right\}, \quad (15)$$

where we define  $k$ -dependent effective time step by

$$\Delta t_{eff}^{PFC}(k, \Delta t) \equiv \frac{\Delta t}{1 + \Delta t k^2 [(r + 1)(1 - a_1) + 2k^2(a_2 - 1) + k^4(1 - a_3)]} \quad (16)$$

For SH Equation, the effective time step is

$$\Delta t_{eff}^{SH}(k, \Delta t) \equiv \frac{\Delta t}{1 + \Delta t [(r + 1)(1 - a_1) + 2k^2(a_2 - 1) + k^4(1 - a_3)]}. \quad (17)$$

$\Delta t_{eff}(k, \Delta t)$  is an effective time step for a mode  $k$ , corresponding to an algorithmic time step  $\Delta t$ . Of particular interest in the case of periodic systems is the dominant mode (the lattice spacing in the PFC model), which, for the scaling choices made in Eq. (2) and Eq. (3) is simply  $k_0 = 1$ . With parameters we employ in the simulation (see next section)  $r = -0.025$ ,  $a_1 = 0.45$ ,  $a_2 = 0.5$ ,  $a_3 = 0.5$ , we obtain the dominant effective time step for both equations

$$\Delta t_{eff}(k_0, \Delta t) = \frac{\Delta t}{1 + 29\Delta t/800}. \quad (18)$$

As  $\Delta t = \infty$ , we obtain the maximum dominant effective time step  $\Delta t_{eff}(k_0, \infty) = 800/29 \approx 27.6$ . We see that a large algorithmic time step  $\Delta t$  does not always translate into a significant amount of system evolution, as the effective time step remains less than 30 for these parameter choices as the algorithmic time step diverges. Thus, this value provides us with an upper bound on our exploration of just how large a algorithmic time step to take, and still obtain accurate results. For example, if we take algorithmic time steps that yields an effective time step  $\Delta t_{eff}(k_0, \Delta t) = \Delta t_{eff}(k_0, \infty)/2 = 400/29$ , then we find  $\Delta t = 800/29$ . In next section, we will show that, when applied to the PFC Equation, this algorithm realizes a significant speedup compared to the traditional Euler algorithm, while maintaining a controlled level of accuracy.

### 3 Numerical results

The simulations were performed in two-dimensions. Fig. 1 shows typical snapshots of simulations for PFC model with parameters  $\phi = 0.07$ ,  $\Delta x = 1.0$ , and

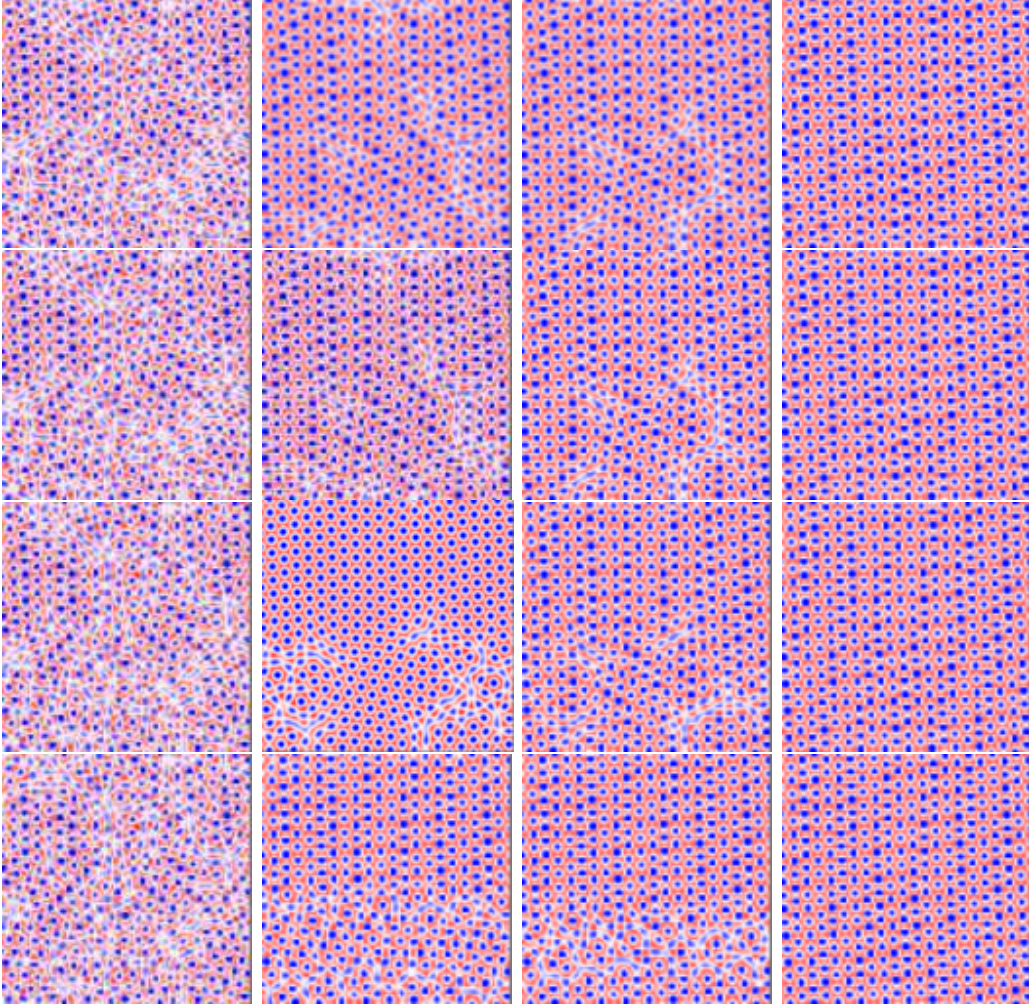


Fig. 1. Snapshots of simulations of the PFC model. Time increases from left to right. The first row shows the field obtained using the Euler algorithm with  $\Delta t_{Eu} = 0, 015$ . The second to bottom rows show the fields obtained employing the unconditionally stable algorithms, with using algorithmic time step  $\Delta t = 3, \Delta t = 10$ , and  $\Delta t = 30$ .

$L_{sys} = 128$  with random initial conditions which corresponds to the liquid state. For comparison, all the simulations start with the same initial condition. The color white represents  $\phi = \bar{\phi}$ , red represents  $\phi = \bar{\phi} + 0.2$  and blue represents  $\phi = \bar{\phi} - 0.2$ . The top row are obtained with Euler algorithm  $\Delta t_{Eu} = 0.015$  at time step  $n = 30000, n = 60000, n = 90000$ , and  $n = 160000$ . All the following rows are obtained by unconditionally stable algorithm  $\Delta t = 3, \Delta t = 10$ , and  $\Delta t = 30$  from the second to bottom row, respectively. For illustration and comparison purposes, we show the system snapshots at the same energy density as the top row — from left, the energy density  $E = 0.002374, E = 0.002360, E = 0.002357$ , and  $E = 0.002350$  from the first to fourth column, respectively. We immediately see that, for the times and energies selected, there are no visible differences between the Euler update simulation and the unconditionally stable algorithm with  $\Delta t = 3$ .

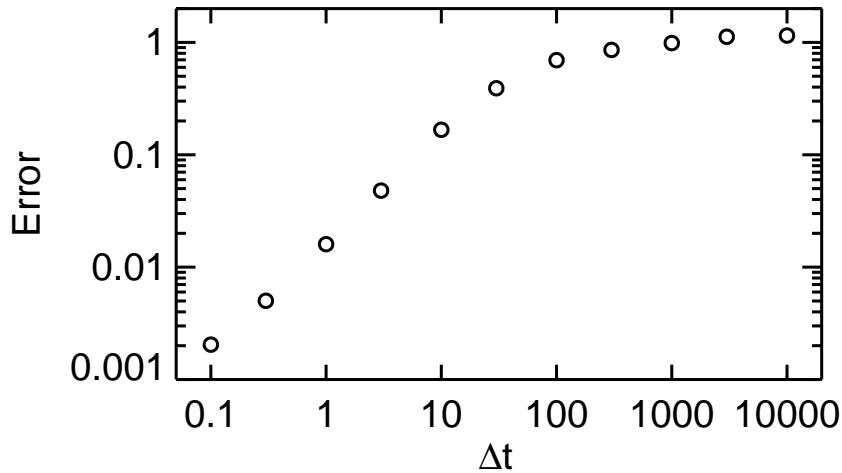


Fig. 2. A measure of the error  $\sqrt{\langle(\phi_{eu} - \phi_{un})^2\rangle/\langle(\phi_{eu} - \bar{\phi})^2\rangle}$  versus the algorithmic time step  $\Delta t$ .

However, there are visible differences between the Euler update and the simulations with  $\Delta t > 3$ . We now wish to make these qualitative observations more quantitative.

To study the accuracy, we compare simulations at the same energy density  $E = 0.002374$  (the first column in Fig. 1). We compute a measure of the error:  $\sqrt{\langle(\phi_{eu} - \phi_{un})^2\rangle/\langle(\phi_{eu} - \bar{\phi})^2\rangle}$ , where  $\phi_{eu}(\mathbf{x})$  denotes the fields obtained using Euler algorithm and  $\phi_{un}(\mathbf{x})$  denotes the fields obtained using the unconditionally stable algorithm. Fig. 2 shows a plot of the error versus a range of algorithmic time steps  $\Delta t$ . The snapshots in Fig. 1 and Fig. 2 indicate that, unsurprisingly, the accuracy decreases as we decrease the algorithmic time step  $\Delta t$ . When  $\Delta t \leq 3$ , the error is below 5%. On the other hand, the error behavior in Fig. 2 for large algorithmic time step  $\Delta t$  tends to saturate, mirroring the saturation in the effective time step  $\Delta t_{eff}^{PFC}$  for dominant mode  $k_0 = 1$ .

Fig. 3 shows a comparison between the dominant effective time step  $\Delta t_{eff}(k_0, \Delta t)$  in Eq. (18) and a numerical estimate of the same quantity. The numerical estimate is obtained by calculating  $t_{Eu}^{tot}/n_{un}$ , where  $t_{Eu}^{tot}$  is the total time needed to reach the final state (a crystalline state without dislocations) using Euler algorithm and  $n_{un}$  is the number of computer steps needed to reach the same state using unconditionally stable algorithms. We find good agreement for  $\Delta t \leq 3$ , while for  $\Delta t > 3$ , the separation between the analytic and numerical expressions increases. While the agreement at small times steps is unsurprising, the curve provides a useful metric for the optimum algorithmic time step, for these parameters, of  $\Delta t \approx 3$ . For this choice, the ratio of the number of time steps needed achieve a particular energy using the unconditionally stable



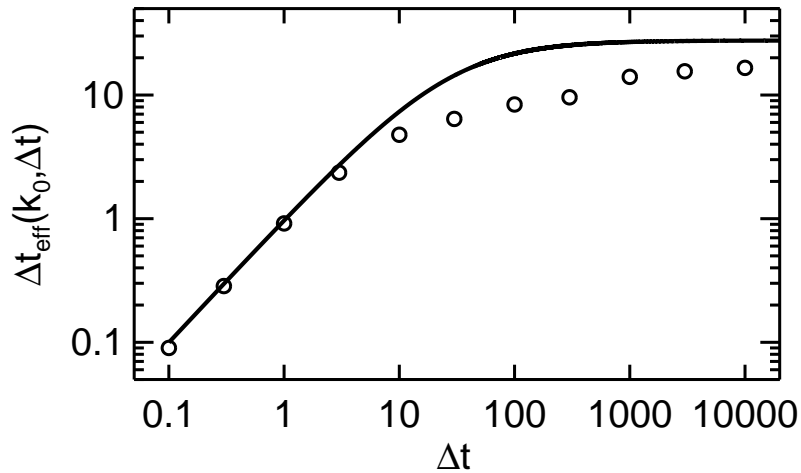


Fig. 3. A comparison between the theoretical dominant effective time step (solid line) and the numerical estimate of the same quantity (circle).

versus Euler algorithm is approximately 180 (the ratio of the dominant mode effective time step to the Euler time step). This is a substantial speedup, and requires minimal analysis to implement the technique.

## 4 Conclusions

In this paper, we have presented an unconditionally stable algorithm for implementation of finite difference solution to the PFC Equation, and demonstrate that a fixed algorithmic time step driving scheme provides significant speedup compared with Euler algorithm with controlled accuracy. For the representative parameters chosen, a speedup of a factor of 180 was obtained. The analytical results and the numerical results are consistent with an effective time step analysis. Although this algorithm allows arbitrarily large algorithmic time steps, one should be cautious that too large a algorithmic time step will make the system evolution inaccurate. Additionally, we demonstrated that the systems energy (and the corresponding microstructures) evolution is governed by the effective time step, which saturates as the algorithmic time step increases, suggesting that there is little advantage in too large an algorithmic time step. A method for obtaining a reasonable value for the algorithmic time step  $\Delta t$  is suggested, in which a few test cases are run with different values of  $\Delta t$  to see which one offers a good speedup and maintains the desired accuracy. The analytic form of the effective time step provides a useful guide for deciding how large a time step to select when trading off the obtainable speedup versus the loss of accuracy.

The unconditionally stable algorithms discussed herein can be readily applied to other systems. Its application to SH Equation is straightforward due to the similarity with the PFC model. There are many other systems, such as diblock copolymers, where there is a dominant mode at late scaling regime. We expect the methodology developed in this paper could find extensive application in non-equilibrium systems.

## References

- [1] J. S. Langer, in *Solids far from Equilibrium*, edited by C. Godrèche (Cambridge University Press, 1992), pp. 297.
- [2] A. J. Bray, Theory of phase-ordering kinetics, *Adv. Phys.* **43**, 357 (1994).
- [3] J. D. Gunton, M. San Miguel and P. S. Sahni, in *Phase Transitions and Critical Phenomena*, Vol. 8, edited by C. Domb and J. L. Lebowitz (New York Academic Press, 1983) pp. 267.
- [4] H. Furukawa, Dynamic scaling assumption for phase separation, *Adv. Phys.*, **34**, 703 (1985).
- [5] J. W. Cahn and J. E. Hilliard, Free energy of a nonuniform system. I. Interface free energy, *J. Chem. Phys.* **28**, 258 (1958).
- [6] S. M. Allen and J. W. Cahn, A microscopic theory for antiphase boundary motion and its application to antiphase domain coarsening, *Acta Metall.* **27**, 1085 (1979).
- [7] P. Wiltzius and A. Cumming, Domain growth and wetting in polymer mixtures, *Phys. Rev. Lett.* **66**, 3000 (1991).
- [8] R. F. Shannon, S. E. Nagler, C. R. Harkless and R. M. Nicklow, Time-resolved x-ray-scattering study of ordering kinetics in bulk single-crystal  $\text{Cu}_3\text{Au}$ , *Phys. Rev. B* **46**, 40 (1992).
- [9] B. D. Gaulin, S. Spooner and Y. Morii, Kinetics of phase separation in  $\text{Mn}_{0.67}\text{Cu}_{0.33}$ , *Phys. Rev. Lett.* **59**, 668 (1987).
- [10] N. Mason, A. N. Pargellis and B. Yurke, Scaling behavior of two-time correlations in a twisted nematic liquid crystal, *Phys. Rev. Lett.* **70**, 190 (1993).
- [11] I. Chuang, N. Turok and B. Yurke, Late-time coarsening dynamics in a nematic liquid crystal, *Phys. Rev. Lett.* **66**, 2472 (1991).
- [12] P. Laguna and W. H. Zurek, Density of Kinks after a Quench: When Symmetry Breaks, How Big are the Pieces?, *Phys. Rev. Lett.* **78**, 2519 (1997).
- [13] K. R. Elder, M. Katakowski, M. Haataja, and M. Grant, Modeling Elasticity in Crystal Growth, *Phys. Rev. Lett.* **88**, 245701 (2002).

- [14] K. R. Elder and M. Grant, Modeling elastic and plastic deformations in nonequilibrium processing using phase field crystals, *Phys. Rev. E* **70**, 051605 (2004).
- [15] J. Swift and P. C. Hohenberg, Hydrodynamic fluctuations at the convective instability, *Phys. Rev. A* **15**, 319 (1977).
- [16] W. H. Shih, Z. Q. Wang, X. C. Zeng, and D. Stroud, Ginzburg-Landau theory for the solid-liquid interface of bcc elements, *Phys. Rev. A* **35**, 2611 (1987).
- [17] K.-A. Wu, A. Karma, J. J. Hoyt, and M. Asta, Ginzburg-Landau theory of crystalline anisotropy for bcc-liquid interfaces, *Phys. Rev. B* **73**, 094101 (2006).
- [18] T. M. Rogers, K. R. Elder and R. C. Desai, Numerical study of the late stages of spinodal decomposition, *Phys. Rev. B* **37**, 9638 (1988).
- [19] Y. Oono and S. Puri, Study of phase-separation dynamics by use of cell dynamical systems. I. Modeling, *Phys. Rev. A* **38**, 434 (1998).
- [20] L. Q. Chen and J. Shen, Applications of semi-implicit Fourier-spectral method to phase field equations, *Comput. Phys. Commun.* **108**, 147 (1998).
- [21] J. Zhu, L. Q. Chen, J. Shen and V. Tikare, Coarsening kinetics from a variable-mobility Cahn-Hilliard equation: Application of a semi-implicit Fourier spectral method, *Phys. Rev. E* **60**, 3564 (1999).
- [22] D. J. Eyre, in *Computational and Mathematical Models of Microstructural Evolution*, edited by J. W. Bullard *et al.* (The Material Research Society, Warrendale, PA, 1998), pp. 39-46.
- [23] B. P. Vollmayr-Lee and A. D. Rutenberg, Fast and accurate coarsening simulation with an unconditionally stable time step, *Phys. Rev. E* **68**, 66703 (2003).
- [24] M. Cheng and A. D. Rutenberg, Maximally fast coarsening algorithms, *Phys. Rev. E* **72**, 055701(R) (2005).
- [25] M. Cheng and J. A. Warren, Controlling the accuracy of unconditionally stable algorithms in Cahn-Hilliard Equation, cond-mat/0609354.